Analyst

Accepted Manuscript

ROYAL SOCIETY OF CHEMISTRY

www.rsc.org/analyst

Label-free electrochemical immunosensor based on ionic organic molecule and chitosan-stabilized gold nanoparticles for the detection of cardiac troponin T

Daniela Brondani,*[a] Jamille Valéria Piovesan,[b] Eduard Westphal,[c] Hugo Gallardo,[c] Rosa Amalia Fireman Dutra,[d] Almir Spinelli [b] and Iolanda Cruz Vieira*[a]

[a] *Laboratory of Biosensors, Department of Chemistry, Federal University of Santa Catarina, 88040-900, Florianópolis, SC, Brazil.*

**E-mail address: danielabrondani@hotmail.com (D. Brondani); iolanda.vieira@ufsc.br (I. C. Vieira).* Phone: + 55 48 3721 6844; Fax: + 55 48 3721 6850.

[b] *Group of Studies of Electrochemical and Electroanalytical Processes, Department of Chemistry, Federal University of Santa Catarina, 88040-900, Florianópolis, SC, Brazil.*

[c] *Laboratory of Synthesis of Liquid Crystals, Department of Chemistry, Federal University of Santa Catarina, 88040-900, Florianópolis, SC, Brazil.*

[d] *Biomedical Engineering Laboratory, Technology Center, Federal University of Pernambuco, 50670-901, Recife, PE, Brazil.*

Abstract

A label-free electrochemical immunosensor based on an ionic organic molecule ((*E*)-4-[(4-decyloxyphenyl)diazenyl]-1-methylpyridinium iodide) and chitosan-stabilized gold nanoparticles (CTS-AuNP) was developed for the detection of cardiac troponin T (cTnT). The new ionic organic molecule was strategically employed as a redox probe, and CTS-AuNP were applied as a "green" platform for the immobilization of the monoclonal anti-cTnT antibody, for the construction of the immunosensor. The characterization of the proposed immunosensor was carried out employing cyclic and square-wave voltammetry and electron microscopy. The film of ionic organic molecules acts as a redox probe and from its electrochemical response the presence of cTnT antigens, which interact specifically with anti-cTnT antibody immobilized on the surface of the immunosensor, can be detected. This interaction results in a decrease in the analytical signal, which is proportional to the amount of cTnT antigens present in the sample analyzed. Under optimized conditions, using square-wave voltammetry (frequency of 100 Hz, amplitude of 100 mV and increment of 8 mV) and an incubation time of 10 min, the proposed immunosensor showed linearity in the range of 0.20 to 1.00 ng mL^{-1} cTnT, with a calculated limit of detection of 0.10 ng mL^{-1}. The proposed immunosensor shows some advantages when compared to other sensors reported in the literature, especially with regard to the detection limit and the time of incubation. A study of the interday precision (n = 8) showed a coefficient of variation of 3.33%. The potential interference of some compounds (glucose, ascorbic acid, albumin, uric acid, creatine, creatinine) on the response of the immunosensor was evaluated and the inhibition of the immunosensor response was found to be less than 8.0%. The immunosensor was successfully used for the determination of cTnT in samples of simulated blood serum with a relative error of <13.0%. Furthermore, the proposed methodology provides a working range that allows the detection of cTnT antigens at levels below the cutoff value used for the diagnosis of acute myocardial infarction and was also found to be faster than the conventional methods.

Keywords: label-free immunosensor; cardiac troponin T; ionic organic molecule; gold nanoparticle.

Introduction

Cardiovascular diseases are frequent causes of patient attendance and admission at emergency medical departments and are a major cause of mortality and morbidity worldwide.[1] The rapid, simple and accurate diagnosis of acute coronary syndromes, such as acute myocardial infarction (AMI), is essential to saving the patient's life. The monitoring of cardiac biomarkers is a key tool in the fight against cardiovascular disease, aiming to deliver a successful prognosis and help in the selection of effective therapies.[2,3] The acute events in cardiovascular diseases have been successfully diagnosed by monitoring established biochemical markers, such as creatine kinase MB, myoglobin and cardiac troponins I and T.[2-5] Cardiac troponin T (cTnT) is widely used as a specific biomarker for myocardial tissue, being considered the “gold standard” for the serological diagnosis and prognosis of AMI due to its high sensitivity and specificity.[6-8] During heart infarction, cTnT is immediately released into the bloodstream. Therefore, the rapid and accurate monitoring of this biomarker could improve the quality of patient care.[3]

Electrochemiluminescence immunoassay (ECLIA) and enzyme-linked immunosorbent assay (ELISA) are the methods generally used for cTnT detection. However, these are not portable and require procedures that can only be carried out in a clinical laboratory, which is clearly inappropriate for a rapid diagnostic in the case of a cardiac emergency.[9] Alternative methods are based on sophisticated chromatographic or electrophoretic procedures,[10,11] which are expensive and also unsuitable for point-of-care testing.

Label-free electrochemical immunosensors are interesting alternatives for this application, particularly due to the speed of analysis and the possibility of miniaturizing the analytical devices to allow portability. For this reason, novel materials such as metal nanoparticles,[12-14] graphene,[15] carbon nanotubes,[9] polymers,[16] surfactants[12] and liquid crystal[14] have been employed for the development of immunosensors with high analytical performance. Metal nanoparticles have been used to increase the rate of electron transfer in electrochemical biosensors. Also, the dimensional similarities of nanomaterials and biomolecules allow the generation of hybrid systems and the formation of nano-connectors for biorecognition events.[17,18] The use of ionic liquid crystals in the development of label-free immunosensors was first explored by our group,[14] and proved to be a very promising material. Liquid crystals are a well-known

class of materials that simultaneously show fluidity and molecular organization, besides exhibiting fascinating electrical and optical properties.[19,20] Films of electroactive organic molecules, which present liquid crystalline properties, can provide sensor platforms that operate based on changes in the electrochemical properties of the immunosensor interface, directly obtained during the antigen-antibody interaction.

This paper describes the synthesis, characterization and full thermal profile of the new ionic organic molecule (*E*)-4-[(4-decyloxyphenyl)diazenyl]-1-methylpyridinium iodide (abbreviated as I-Py) and its application together with chitosan-stabilized gold nanoparticles (CTS-AuNP) in the development of a label-free electrochemical immunosensor for cardiac troponin T (cTnT). This immunosensor was optimized and then applied in the detection and quantification of cTnT in samples of simulated blood serum.

Experimental

Reagents and solutions

Human cardiac troponin T (cTnT), monoclonal anti-cTnT, chloroauric acid ($HAuCl_4$), chitosan (low molecular weight, 80% deacetylation), glycine, lysine, creatine, creatinine, uric acid, bovine serum albumin (BSA), citric acid, glucose and ascorbic acid were obtained from Sigma-Aldrich. All reagents were of analytical grade and were used without further purification, and all aqueous solutions were prepared in ultrapure water obtained from a Milli-Q system (Millipore, USA) with a resistivity of 18.2 MΩ cm^{-1}. Phosphate buffer saline (PBS) solution (0.01 mol L^{-1}, pH 7.4), used as the supporting electrolyte in the voltammetric measurements taken with the immunosensor, was prepared by dissolving KCl, NaCl, Na_2HPO_4 and KH_2PO_4 in ultrapure water. The studies to evaluate the effect of pH on the electrochemical process of the I-Py modified electrode were conducted in acetate buffer solution (0.1 mol L^{-1}, pH 4.0 and 5.0) and phosphate buffer solution (0.1 mol L^{-1}, pH 6.0, 7.0 and 8.0). A solution of simulated blood serum was prepared by mixing the following reagents (modified version of Krebs):[21] glycine (1.8 mg), lysine (3.0 mg), creatine (1.1 mg), creatinine (0.4 mg), uric acid (4.1 mg), BSA (4.0 mg), citric acid (2.5 mg), glucose (83.0 mg) and ascorbic acid (0.5 mg), in 100.0 mL of PBS (0.01 mol L^{-1}, pH 7.4). Thin layer chromatography (TLC) was carried out using silica-gel Si 60-F254 (Merck). Purifications were carried out by

recrystallization using commercial grade solvents and by column chromatography on silica-gel 60-200 mesh 60A (Acros).

Instrumentation

Electrochemical measurements using cyclic voltammetry (CV) and square-wave voltammetry (SWV) were performed in an Autolab PGSTAT101 potentiostat/galvanostat (Eco Chemie, The Netherlands), operating with data processing software (NOVA, software version 1.10). All voltammetry experiments were carried out using a conventional three-electrode system: the immunosensor as the working electrode, a platinum plate as the auxiliary electrode and Ag/AgCl (3.0 mol L^{-1} KCl) as the reference electrode. Spectrophotometric measurements were performed on a Cary 60 UV-Vis spectrometer (Agilent Technologies, USA). Zeta potential measurements were performed using a Zetasizer Nano ZS system (Malvern Instruments, UK). Transmission electronic microscopy (TEM) analysis was performed with a JEOL JEM-1011 transmission electron microscope operating at 100 keV. Scanning electron microscopy was performed using a JEOL JSM-6701 field emission gun (FEG-SEM) microscope (accelerating voltage of 10 keV). The micrographs were obtained at the Central Laboratory of Electron Microscopy at the Federal University of Santa Catarina (Florianópolis, Brazil).

Infrared spectra were recorded on a Perkin-Elmer model 283 spectrometer. ^{1}H and ^{13}C NMR spectra were recorded with a Varian Mercury Plus spectrometer operating at 400 and 100.6 MHz, respectively, or, when described, with a Bruker AC-200F spectrometer operating at 200 and 50.4 MHz, respectively. Thermal transitions were determined by differential scanning calorimetry (DSC) measurements carried out using TA equipment with a Q2000 module applying a heating/cooling rate of 10 °C min^{-1} and a nitrogen flow of 50 mL min^{-1}. Thermal stability was investigated by thermogravimetric analysis (TGA) using a Shimadzu analyzer with a TGA-50 module applying a heating rate of 10 °C min^{-1} and nitrogen flow of 20 mL min^{-1}. Melting points and mesomorphic textures were determined using an Olympus BX50 microscope equipped with a Mettler Toledo FP-82 Hot Stage and an Olympus DP73 digital camera. Elemental analysis was carried out using a Carlo Erba model E-1110 instrument.

Synthesis and characterization of ionic organic molecule I-Py

The new ionic organic compound was synthesized by a simple and high yielding protocol, as described in Scheme 1. The synthetic protocol and full characterization of the intermediates **2** and **3** have been previously described in the literature.[14] The final reaction, *i.e.*, the methylation of pyridine, was carried out by mixing and heating the two reactants together in the presence of acetonitrile as the solvent. The desired ionic product (**I-Py**) was obtained in high yields and its structure and purity were fully characterized by IR, ^{1}H and ^{13}C NMR and elemental analysis (For IR, ^{1}H and ^{13}C spectra, see Fig. S1, S2 and S3 in the Supplementary Information).

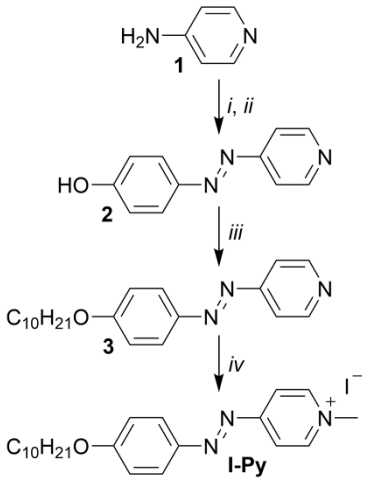

Scheme 1. Synthetic route for the ionic organic compound **I-Py**.

Synthesis Protocol

(*E*)-**4-[(4-decyloxyphenyl)diazenyl]-1-methylpyridinium iodide** (**I-Py**)

The reagents 4-[(4-decyloxyphenyl)diazenyl] pyridine (**3**) (0.80 g; 2.36 mmol), iodomethane (0.74 mL; 11.8 mmol) and acetonitrile (40 mL) were placed in a round-bottomed flask and the mixture was maintained at 70 °C under stirring for 20 h. The solution was cooled to room temperature and the solvent and excess iodomethane were removed under reduced pressure. Maceration in boiling heptane yielded 1.09 g (96%) of the pure ionic azo compound as a dark red solid. **m.p.**: Cr – 119 °C – SmA – ≈165 °C – dec. **IR** (KBr) $\nu_{max}cm^{-1}$: 2923, 2867, 2851, 1635, 1601, 1578, 1497, 1472, 1443, 1406, 1320, 1300, 1258, 1208, 1186, 1171, 1138, 1019, 861, 843. **^{1}H NMR** ($CDCl_3$) δ ppm:

0.89 (t, *J* = 6.9 Hz, 3H, -CH_3), 1.20 – 1.40 (m, 12H, -CH_2-), 1.49 (m, 2H, -CH_2-), 1.84 (m, 2H, -$C\underline{H}_2CH_2O$-), 4.09 (t, *J* = 6.6 Hz, 2H, -CH_2O-), 4.74 (s, 3H, Py^+-$C\underline{H}_3$), 7.03 (d, *J* = 9.1 Hz, 2H, Ar-H), 8.00 (d, *J* = 9.1 Hz, 2H, Ar-H), 8.24 (d, *J* = 7.0 Hz, 2H, Py-H), 9.45 (d, *J* = 7.0 Hz, 2H, Py-H). **^{13}C** NMR ($CDCl_3$) δ ppm: 14.37, 22.90, 26.16, 29.24, 29.53, 29.56, 29.77, 32.11, 49.28, 69.19, 115.69, 120.31, 127.99, 147.28, 147.64, 161.04, 165.82. **Elemental Analysis -** calculated for $C_{22}H_{32}IN_3O$: C 54.89; H 6.70; N 8.73%; Found: C 55.07; H 6.94; N 8.85%.

Synthesis and characterization of CTS-AuNP

Chitosan-stabilized gold nanoparticles (CTS-AuNP) were synthesized by the following procedure (modified version of method described by Huang and Yang):[22] 10.0 mL of a 0.25% (w/v) chitosan solution (in aqueous acetic acid 1.0%, v/v) were heated to a temperature of 70 °C. Next, 100 μL of an aqueous $HAuCl_4$ solution (0.1 mol L^{-1}) were added maintaining mechanical stirring for 30 min. A red dispersion was obtained, indicating the formation of AuNP. This CTS-AuNP dispersion was mixed with a solution of anti-cTnT (1000 ng mL^{-1}) in a 1:1 (v/v) ratio, resulting in a purple dispersion, indicating the binding of antibodies to the nanomaterials. The CTS-AuNP-anti-cTnT dispersion obtained was then used for the construction of the proposed immunosensor. Spectrophotometric and zeta potential measurements of the CTS-AuNP and CTS-AuNP-anti-cTnT samples were performed for the characterization of the nanomaterials. In addition, TEM analysis of these samples was carried. For this analysis, the samples were prepared by depositing suspensions onto a carbon-coated copper grid. The grids were placed on filter paper to remove the excess material and allowed to dry in a desiccator. The average particle size was determined by counting approximately 300 particles using ImageJ software.[23]

Construction of the immunosensor

Initially, a glassy carbon electrode (GCE, diameter 2.0±0.1 mm) was polished with 0.05 μm alumina powder on a flat pad for 3 min and rinsed with ultrapure water and ethanol. The GCE was then subjected to ultrasonic cleaning in ultrapure water for 10 min to remove the residual alumina particles. The immunosensor construction involved the following steps: firstly, 4 μL of a solution of I-Py ($4.0x10^{-3}$ mol L^{-1}, in chloroform) were

dropped onto the clean GCE surface and the solvent was allowed to evaporate in a desiccator under vacuum. Next, 3 μL of the CTS-AuNP-anti-cTnT dispersion were dropped on the I-Py film formed, which was again left to dry in a desiccator for a few minutes. Finally, the immunosensor was incubated for 10 min with 3 μL of a solution of glycine (0.1 mol L^{-1}), in order to block non-specific sites on the surface of this sensor, and then washed with PBS (0.01 mol L^{-1}, pH 7.4) to remove the excess protein and dried in a desiccator. The immunosensor was then ready for use. A schematic illustration of the steps involved in the construction of the proposed immunosensor is shown in Scheme 2. FEG-SEM micrographs of the electrode surface were obtained after each step during the immunosensor construction.

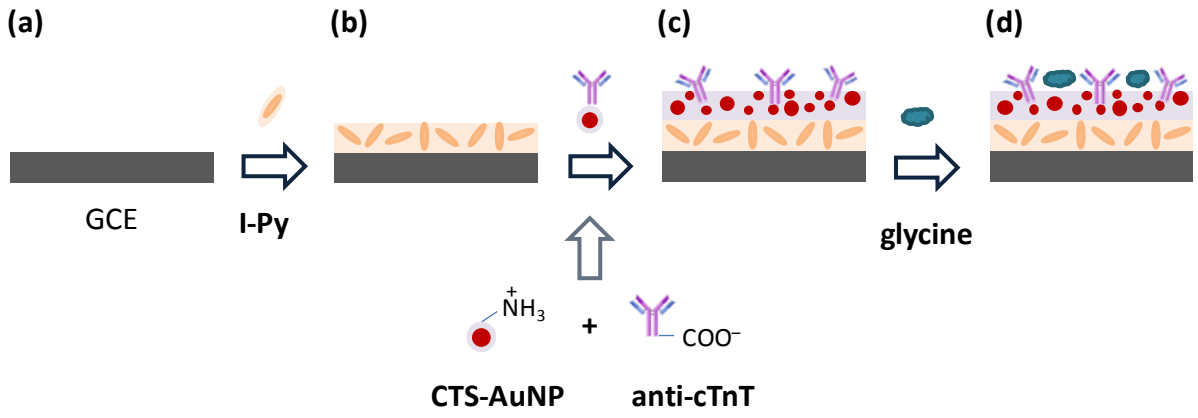

Scheme 2. Schematic illustration of the successive steps involved in the construction of the immunosensor. (a) Bare GCE, (b) formation of the I-Py film, (c) adsorption of the CTS-AuNP with immobilized anti-cTnT antibody and (d) blocking with glycine.

Electrochemical measurements

The optimization and characterization of the proposed immunosensor was carried out employing CV and SWV techniques. The immunosensor was applied in the determination of cTnT in PBS (0.01 mol L^{-1}, pH 7.4) and in simulated serum samples with the use of SWV measurements. For this analysis, the immunosensor was dipped in the supporting electrolyte solution to obtain the base peak (relative to the reduction of the azo group (N=N) of the I-Py molecule immobilized on the sensor) applying a scanning potential of +0.5 to –0.8 V, frequency of 100 Hz , amplitude of 100 mV and increment of 8 mV. Subsequently, 3 μL of the standard solutions or simulated samples containing different concentrations of cTnT were placed on the sensor surface and incubated for 10 min at room temperature, to complete the immunoreaction. After this period, the immunosensor

surface was rinsed with PBS (0.01 mol L^{-1}, pH 7.4) to remove the non-specifically bound cTnT antigens. The immunosensor was again immersed in the electrolyte solution to carrying out the voltammetric measurement. The decrease in the current of the voltammetric response (compared to the base peak) was proportional to the concentration of the cardiac biomarker in the sample.

Results and Discussion

Thermal Characterization of I-Py

The thermal properties of the new compound **I-Py** were investigated by polarized-light optical microscopy (POM), DSC and TGA. On heating, it was observed by POM and DSC that the compound melts at 119 °C to a liquid crystalline phase (for DSC plot see Fig. S4). The presence of an oily streak texture (Fig. 1) and large homeotropic (dark) areas is a strong indication of a SmA phase, which is commonly observed in ionic liquid crystalline materials.[19,24,25] On further heating, the compound begins to decompose before any transition to the liquid state (isotropic liquid) was evident. This was confirmed by TGA, where it was observed that the weight loss (*i.e.*, decomposition process) started at around 165 °C under N_2 atmosphere (for TGA plot, see Fig. S5).

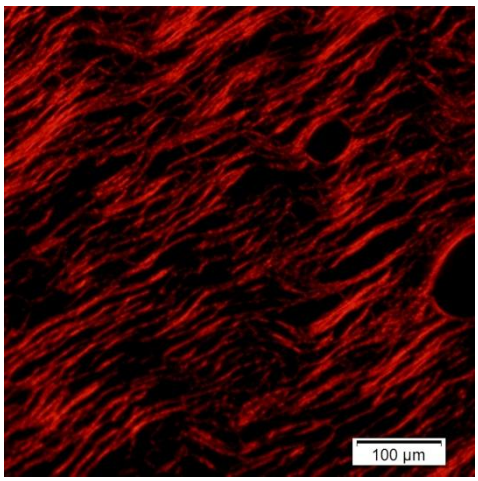

Fig. 1. Oily streak texture observed for compound **I-Py**. Micrograph obtained by POM (under crossed polarizers) on first heating (140 °C).

Interestingly, a crystallization peak was not observed by DSC on cooling. On the second heating scan, before the melting to the SmA phase, an exothermic peak was observed. This peak indicates that during the short period between the two scans the sample remained in a supercooled state and the crystallization process occurred only when the sample was heated again. The POM analysis revealed that, on cooling, the material crystallizes slowly after some time at a temperature close to room temperature, indicating that the supercooled state is only metastable.

Electrochemical behavior of ionic organic molecule I-Py

An investigation to evaluate the influence of the pH of the supporting electrolyte on the electrochemical process of the I-Py modified electrode was conducted in acetate buffer solution (pH 4.0 and 5.0) and phosphate buffer solution (pH 6.0, 7.0 and 8.0) by CV. A redox couple was observed for the I-Py modified electrode when the potential was varied in the range of –0.5 V to 0.3 V, at a scan rate of 100 mV s^{-1}, which was attributed to the azo group conjugated to the aromatic rings of the I-Py structure.[14,26] According to the results shown in Fig. 2, with an increase in pH the peak oxidation and reduction potentials shifted toward more negative values, implying that the electrochemical process involves proton transfer. This study revealed a linear relationship between the formal potential ($E^{0'}$) and the pH values, with a slope of approximately 61.1 mV pH^{-1} (r^2 = 0.997), which is close to that expected for Nernstian systems with electron transfer followed by deprotonation. Thus, as proposed by Zapp *et al.*,[14] the results suggest that the same number of protons and electrons participate in the electrochemical reaction involving the I-Py molecule (see Fig. S6). In addition, the influence of the scan rate on the voltammetric profile for the I-Py modified electrode was also investigated by CV (see Fig. S7 and the description in the Supplementary Information).

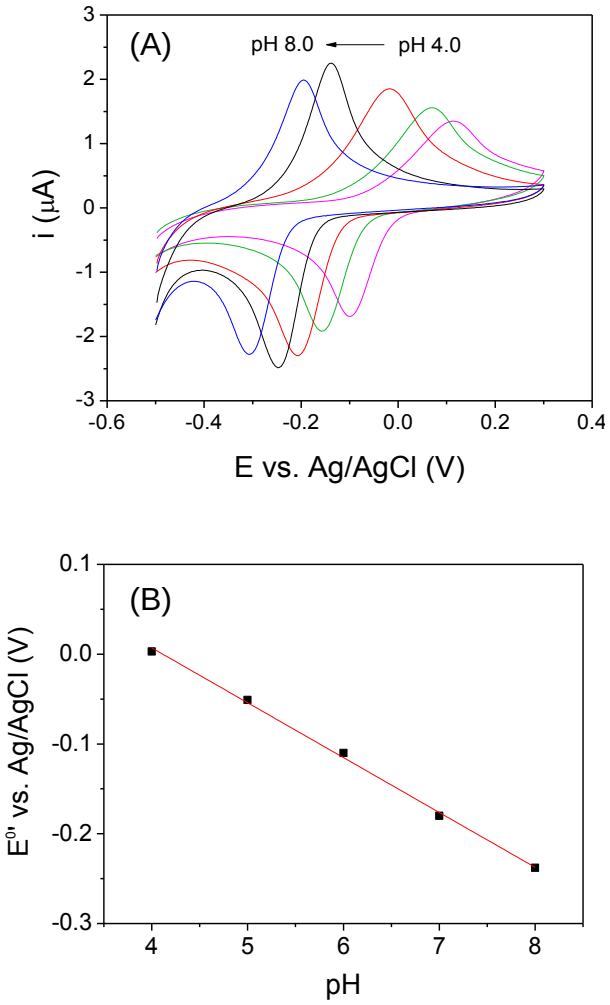

Fig. 2. (A) Cyclic voltammograms of the I-Py modified electrode in different supporting electrolytes: acetate buffer solution (pH 4.0 and 5.0) and phosphate buffer solution (pH 6.0, 7.0 and 8.0), at a scan rate of 100 mV s^{-1}. (B) $E^{0'}$ *vs.* pH.

Immobilization of antibodies and construction of the immunosensor

The synthesis of CTS-AuNP was based on the fundamentals of green chemistry[27] where the CTS biopolymer was used as a stabilizer for the metal nanoparticles and also a reducing agent for the Au(III) solution, eliminating the need for use of other reagents.[28,29] The CTS-AuNP dispersion was stored at 4 °C and no color change was observed after storage for 8 months. The average diameter of the CTS-AuNP was estimated as dm ≈ 13.7±0.7 nm from ensembles of 300 particles found in arbitrarily chosen areas of the enlarged micrographs obtained by TEM (Fig. 3-A). The histogram shows the particle size distributions obtained, which can be reasonably well fitted by a Gaussian curve. The CTS-AuNP dispersion was then mixed with the anti-cTnT and a change in the dispersion color from red to purple was observed due to a

shift in the plasmon band from 526 to 546 nm (see Fig. S8). The prominent shift in the plasmon band of AuNP can be attributed to the "aggregation" of nanoparticles induced by the presence of protein,[30-32] as can be seen in Fig. 3. The TEM images indicated an approximation of the AuNP, due to interaction with the macromolecules of the protein (anti-cTnT), with no significant change in the particle size (dm ≈ 12.7±0.2 nm) (Fig. 3-B). This suggests that the antibodies were immobilized on the CTS-AuNP, probably through the interaction between the protonated NH_2-terminal groups of the CTS (which coats the surface of the metal nanoparticles) and the deprotonated COOH-terminal groups of the anti-cTnT antibody. This proposal was corroborated by the zeta potential measurements, which indicated an average potential of +60.6 mV at the surface of the CTS-AuNP and +43.2 mV for CTS-AuNP with anti-cTnT antibody immobilized. The FEG-SEM images, which are presented below, also contributed to the assertion that there was an effective immobilization of antibodies. The proposed methods for the synthesis of the AuNP and immobilization of the antibody involve simple, rapid and low cost procedures and the resulting materials are expected to be non-toxic and biocompatible.

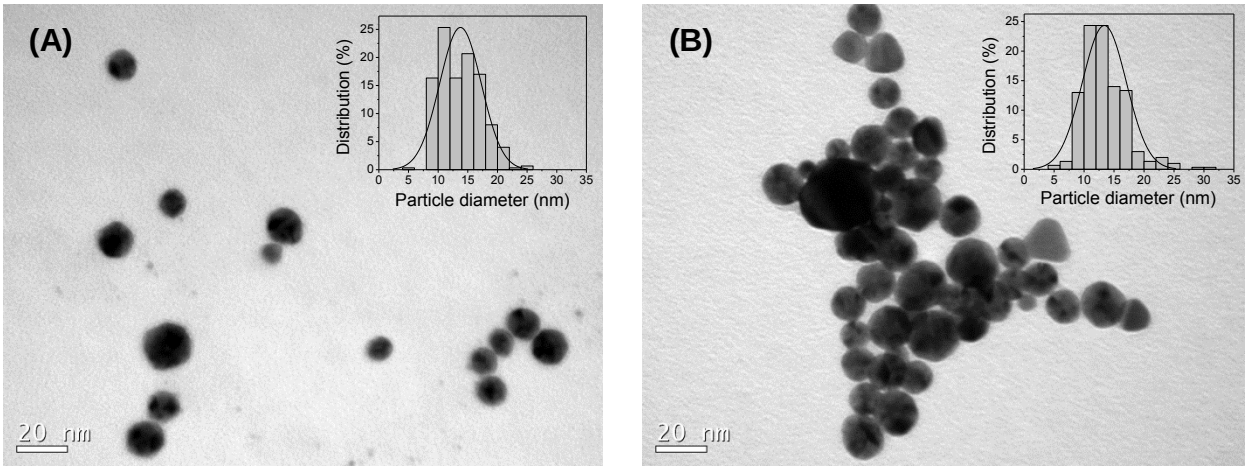

Fig. 3. TEM micrographs of the CTS-stabilized AuNP (A) before and (B) after addition of anti-cTnT. The insets show the particle size histogram based on approximately 300 particles.

Fig. 4 shows the images of the sensor surfaces obtained by FEG-SEM in each step of the immunosensor construction. Fig. 4-A shows the surface of a bare GCE, and Fig. 4-B shows the GCE surface coated with I-Py film, which presents a rough texture (bright parts) with the almost uniform presence of holes (dark parts, possibly not coated). In Fig. 4-C it can be observed that the domains of CTS-AuNP (bright spots) are

homogeneously distributed in the I-Py film. In Fig. 4-D the anti-cTnT antibodies are immobilized on the CTS-AuNP, shown through the change in the shape of the bright spots (AuNP). This image clearly exhibits the presence of numerous small conjugates on the sensor surface, which reinforces the affirmation that the antibodies are strongly immobilized on the CTS-AuNP (thus resisting the successive washing steps).

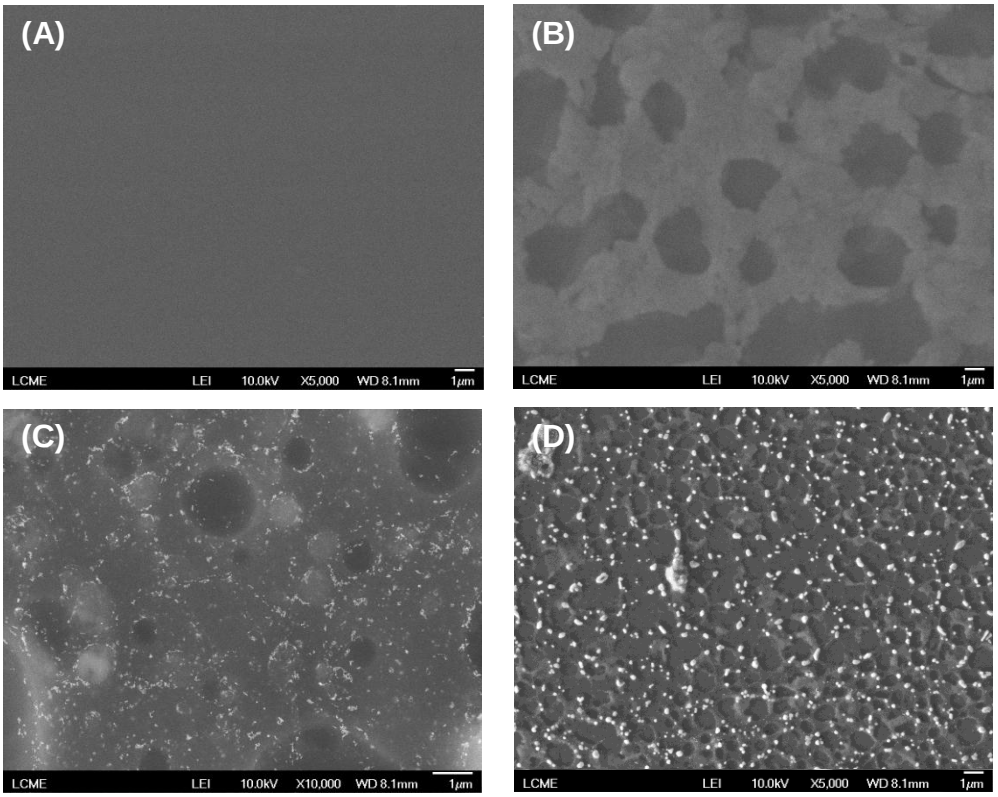

Fig. 4. FEG-SEM micrograph of the (A) bare GCE (B) GCE/I-Py, (C) GCE/I-Py/CTS-AuNP and (D) GCE/I-Py/CTS-AuNP-anti-cTnT samples observed at 10.0 kV.

Functioning of the immunosensor

The molecules of I-Py were strategically employed at the sensing platform interface to develop a label-free immunosensor. Thus, the I-Py film acts as a redox probe and from its electrochemical response (peak current) the presence of cTnT antigens, which interact specifically with anti-cTnT antibody immobilized on the surface of the immunosensor, can be detected. This interaction results in a decrease in the analytical signal, which is proportional to the amount of cTnT antigens present in the sample analyzed, since the protein which binds to the sensor platform hinders the transfer of electrons.

Fig. 5 shows the square wave voltammograms obtained in each step of the immunosensor construction. All voltammograms were obtained in a PBS solution (0.01 mol L^{-1}, pH 7.4). The voltammogram "a" was obtained using a GCE coated with the I-Py film, in which a peak reduction of the azo group (N=N) of the I-Py molecules can be observed. This peak was used as a “base peak” for the detection and quantification of interactions occurring between the antigen and antibody on this sensor platform. The voltammogram "b" refers to the GCE coated firstly with a film of I-Py and secondly with a film of CTS-AuNP-anti-cTnT, from which a significant decrease in the peak current of I-Py in relation to the voltammogram "a" can be observed due to the presence of CTS and immobilized antibodies, which significantly hinder the charge transfer at the electrode surface. The voltammogram "c" also showed a small decrease in the current caused by the blockade with glycine, used to prevent nonspecific binding. The voltammogram “d” was obtained after the immunosensor constructed was incubated with a solution of cTnT antigens for a certain time interval, in order to allow specific binding of these antigens with the anti-cTnT antibodies immobilized on the electrode surface. This led to the presence of an increasing amount of protein on the electrode surface and hence a decrease in the electron transfer and also in the peak current of I-Py. This decrease is proportional to the amount of antigen bound to the immunosensor surface, which in turn is equivalent to the concentration of the antigen in the solution, allowing the quantification of these highly specific proteins.

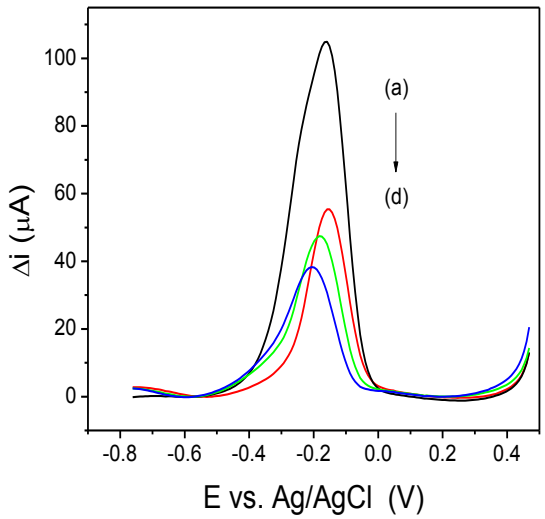

Fig. 5. Square wave voltammograms obtained after each step during the construction of the immunosensor: (a) GCE/I-Py; (b) GCE/I-Py/CTS-AuNP-anti-cTnT and (c) GCE/I-Py/CTS-AuNP-anti-cTnT/glycine. The voltammogram (d) was obtained with the proposed immunosensor after incubation (10 min) in the cTnT solution. All voltammetric measurements were obtained in a PBS solution (0.01 mol L^{-1}, pH 7.4).

Optimization of the proposed immunosensor

In order to optimize the construction of the immunosensor and the experimental conditions, some parameters were investigated using SWV. The initial parameters investigated were the quantities of I-Py and CTS-AuNP-anti-cTnT used in the formation of films on the surface of the GCE. After optimization of the construction of the immunosensor, the SWV parameters (frequency, amplitude and increment) were varied in order to obtain the best immunosensor performance. Also, in the immunoassays the incubation time was investigated. The ranges studied for each parameter and the best results obtained are shown in Table 1.

Table 1. Optimization parameters of the proposed immunosensor

Parameter	Range studied	Best response
I-Py (nmol)	8.0 – 24.0	16.0
CTS-AuNP-anti-cTnT (µL)	2.0 – 6.0	3.0
Frequency (Hz)	10 – 100	100
Amplitude (mV)	10 – 100	100
Increment (mV)	1 – 10	8
Incubation time (min)	5 – 20	10

Analytical performance of the immunosensor

After optimization of the immunosensor construction, the parameters of the SWV technique and the incubation time, a calibration curve was constructed using the standard solution of cTnT in PBS solution (0.01 mol L^{-1}, pH 7 4). Fig. 6 shows the inhibition curve for the response obtained using the proposed immunosensor under optimized conditions after incubation with different concentrations of the cTnT standard solution (analysis performed in triplicate). The curve showed linearity in the range of 0.20 to 1.00 ng mL^{-1} cTnT, and the regression equation is as follows: % inhibition = -7.08 + 61.47 [cTnT], with a correlation coefficient (r^2) of 0.985. The calculated limit of detection (LOD = 3 x standard deviation of the intercept / slope) was approximately 0.10 ng mL^{-1}. A study of the interday precision (n = 8) was performed with the proposed immunosensor, which showed a coefficient of variation of 3.33%, using a concentration of 0.60 ng mL^{-1} of cTnT.

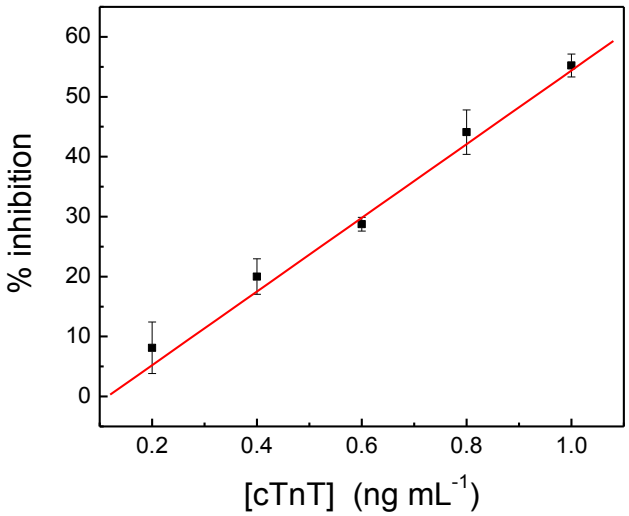

Fig. 6. Calibration curve: inhibition of response obtained using the proposed immunosensor, under optimized conditions, in PBS solution (0.01 mol L^{-1}, pH 7.4), after incubation (10 min) with different concentrations of cTnT standard solution.

The World Health Organization (WHO) establishes the recommended level of cTnT in blood as ≤ 0.01 ng mL^{-1} for healthy individuals, and ≥ 0.3 ng mL^{-1} as the criterion for the diagnosis of acute myocardial infarction (AMI) based on this biomarker.[13] The proposed immunosensor proved to be sufficiently sensitive to measure the concentration of cTnT below the "cutoff point" for the diagnosis of AMI, besides being faster than conventional methods (e.g., ELISA). Furthermore, the proposed immunosensor shows some advantages when compared to other sensors reported in the literature (Table 2), especially with regard to the detection limit and the time of incubation.

Table 2. Analytical performance of different immunosensors for troponin detection

Sensor	Method	Linear range	Incubation time (min)	LOD	Reference
Nanostructured film based on polyethyleneimine and carboxylated carbon nanotubes on gold electrode **(cTnT)**	Electrochemical	0.1 – 10.0 ng mL^{-1}	60	0.033 ng mL^{-1}	[9]
Immunosensor based on gold nanoparticles co-immobilized on a dithiol-modified gold surface **(cTnT)**	Piezoelectric	0.1 – 0.5 ng mL^{-1}	15	0.0015 ng mL^{-1}	[13]
Gold nanoparticles deposited on screen printed electrodes **(cTnI)**	Capacitance	–	15	0.2 ng mL^{-1}	[33]
Aminobenzoic acid film-based immunoelectrode **(cTnT)**	Amperometric	0.05 - 5.0 ng mL^{-1}	60	0.016 ng mL^{-1}	[34]
Microchip with the surface-functionalized poly(dimethylsiloxane) **(cTnI)**	Electrochemical	0.2 – 10.0 ng mL^{-1}	8	0.148 ng mL^{-1}	[35]
Self-assembled monolayer (SAM) on Au **(cTnT)**	Surface plasmon resonance	< 50 μg mL^{-1}	2	100 ng mL^{-1}	[36]
Streptavidin-microsphere modified screen-printed electrode surface **(cTnT)**	Electrochemical	0.1 – 10.0 ng mL^{-1}	120	0.2 ng mL^{-1}	[37]
Immunosensor based on ionic organic molecule and chitosan-stabilized gold nanoparticles **(cTnT)**	Electrochemical	0.2 – 1.0 ng mL^{-1}	10	0.1 ng mL^{-1}	This study

Study of potential interference and application of immunosensor

The potential interference of some compounds, including the PBS solution (0.01 mol L^{-1}, pH 7.4), glucose (830.0 mg L^{-1}), ascorbic acid (5.0 mg L^{-1}), BSA (40.4 mg L^{-1}), uric acid (40.5 mg L^{-1}), creatine (10.7 mg L^{-1}), creatinine (4.2 mg L^{-1}) and simulated blood plasma (containing a mixture of constituents) on the response of the immunosensor was evaluated as described in the *Experimental Section*). The results obtained in this study showed that the inhibition of the immunosensor response was less than 8.0%, indicating that it is possible to perform the determination of cTnT in the presence of these potential interferents without significant interference.

The proposed immunosensor was used for the determination of cTnT in two samples (A and B) of simulated blood serum spiked with different concentrations of antigen (0.60 and 0.80 ng mL^{-1}). The results obtained are shown in Table 3, demonstrating that the proposed methodology is viable for determination of cTnT in the presence of interfering compounds with an acceptable relative error.

Table 3. Determination of cardiac troponin T (cTnT) in samples of simulated blood serum using the proposed immunosensor

Sample	*[cTnT] added (ng mL^{-1})*	*[cTnT] detected (ng mL^{-1})**	*Relative error (%)*
A	0.60	0.65 ± 0.04	8.3
B	0.80	0.90 ± 0.03	12.5

* n = 3

CONCLUSIONS

The label-free immunosensor based on a new ionic organic molecule showed important characteristics, such as adequate interday precision (repeatability), low interference from the blood serum constituents and rapid construction. Furthermore, the proposed methodology provides a working range (0.20 to 1.00 ng mL^{-1} cTnT) that allows the detection of cTnT antigens at levels below the cutoff value used for the diagnosis of AMI and was also found to be more sensitive and faster than the conventional methods (e.g., ELISA). The proposed immunosensor also offers advantages when compared to other immunosensors for troponin detection reported in the literature, especially with regard to the time of incubation (10 min), which is among the lowest ever achieved, together with a good limit of detection (0.10 ng mL^{-1}). Thus, the results of this study indicate that the proposed immunosensor is feasible for AMI diagnosis, although further assays with real samples need to be performed before its clinical application.

Acknowledgments

Financial support from FAPESC/CNPq (Process 2807/2012 – PRONEM) and also the scholarships granted by CNPq to JP, as well as financial support from CAPES-Brazil to DB and EW, are gratefully acknowledged. Research supported by Central

Laboratory of Electron Microscopy, Federal University of Santa Catarina (Florianópolis, Brazil).

References

1. S. Mendis, K. Thygesen, K. Kuulasmaa, S. Giampaoli, M. Mahonen, K. Ngu Blackett and L. Lisheng, *Int. J. Epidemiol.*, 2011, **40**, 139–146.
2. B. McDonnell, S. Hearty, P. Leonard and R. O'Kennedy, *Clin. Biochem.*, 2009, **42**, 549–561.
3. A. Qureshi, Y. Gurbuz and J. H. Niazi, *Sens. Actuators, B*, 2012, **171**, 62–76.
4. U. Friess and M. Stark, *Anal. Bioanal. Chem.*, 2009, **393**, 1453–1462.
5. I. Ramasamy, *Clin. Chim. Acta*, 2011, **412**, 1279–1296.
6. J. S. Alpert, K. Thygesen, E. Antman and J. P. Bassand, *J. Am. Coll. Cardiol.*, 2000, **36**, 959–969.
7. F. S. Apple, A. H. B. Wu and A. S. Jaffe, *Am. Heart J.*, 2002, **144**, 981–986.
8. A. A. Mohammed and J. L. Januzzi Jr., *Cardiol. Rev.*, 2010, **18**, 12–19.
9. S. L. R. Gomes-Filho, A. C. M. S. Dias, M. M. S. Silva, B. V. M. Silva and R. F. Dutra, *Microchem. J.*, 2013, **109**, 10–15.
10. S. Ray, P. J. Reddy, S. Choudhary, D. Raghu and S. Srivastava, *J. Proteomics*, 2011, **74**, 2660–2681.
11. L. Denoroy, L. Zimmer, B. Renaud and S. Parrot, *J. Chromatogr., B*, 2013, **927**, 37–53.
12. E. V. Suprun, A. L. Shilovskaya, A. V. Lisitsa, T. V. Bulko, V. V. Shumyantseva and A. I. Archakov, *Electroanalysis*, 2011, **23**, 1051–1057.
13. R. A. S. Fonseca, J. Ramos-Jesus, L. T. Kubota and R. F. Dutra, *Sensors*, 2011, **11**, 10785–10797.
14. E. Zapp, E. Westphal, H. Gallardo, B. Souza and I. C. Vieira, *Biosens. Bioelectron.*, 2014, **59**, 127–133.
15. K. Mao, D. Wu, Y. Li, H. Ma, Z. Ni, H. Yu, C. Luo, Q. Wei and B. Du, *Anal. Biochem.*, 2012, **422**, 22–27.
16. M. I. Prodromidis, *Electrochim. Acta*, 2010, **55**, 4227–4233.
17. S. Guo and S. Dong, *Trends Anal. Chem.*, 2009, **28**, 96–109.
18. Y. Wu, U. Wollenberger, M. Hofrichter, R. Ullrich, K. Scheibner and F. W. Scheller, *Sens. Actuators, B*, 2011, **160**, 1419–1426.

19. K. Binnemans, *Chem. Rev.*, 2005, **105**, 4148–4204.
20. P. F. Lagerwall and G. Scalia, *Curr. Appl. Phys.*, 2012, **12**, 1387-1412.
21. H. A. Krebs, *Annu. Rev. Biochem.*, 1950, **19**, 409–430.
22. H. Huang and X. Yang, *Biomacromolecules*, 2004, **5**, 2340–2346.
23. C. A. Schneider, W. S. Rasbanda and K. W. Eliceiri, *Nat. Methods*, 2012, **9**, 671–675.
24. K. V. Axenov and S. Laschat, *Materials*, 2011, **4**, 206–259.
25. E. Westphal, D. H. D. Silva, F. Molin and H. Gallardo, *RSC Advances*, 2013, **3**, 6442–6454.
26. M. A. El-Attar, I. M. Ismail, M. M. Ghoneim. *J. Braz. Chem. Soc.*, 2012, **23**, 1523–1535.
27. P. T. Anastas and J. C. Warner, *Green Chemistry: Theory and Practice*. Oxford University Press: New York, 1998.
28. H. Huang and X. Yang, *Carbohydr. Res.*, 2004, **339**, 2627–2631.
29. S. Boufi, M. R. Vilar, A. M. Ferraria and A. M. B. do Rego, *Colloids Surf., A*, 2013, 439, 151–158.
30. N. Lala, A. G. Chittiboyina, S. P. Chavan and M. Sastry, *Colloids Surf., A*, 2002, **205**, 15–20.
31. K. Aslan, C. C. Luhrs and V. H. Pérez-Luna, *J. Phys. Chem., B*, 2004, **108**, 15631–15639.
32. N. R. Tiwari, A. Rathore, A. Prabhune and S. K. Kulkarni, *Adv. Biosci. Biotechnol.*, 2010, **1**, 322–329.
33. V. Bhalla, S. Carrara, P. Sharma, Y. Nangia and C. R. Suri, *Sens. Actuators, B*, 2012, **161**, 761–768.
34. A. B. Mattos, T. A. Freitas, L. T. Kubota and R. F. Dutra, *Biochem. Eng. J.*, 2013, **71***,* 97–104.
35. S. Ko, B. Kim, S. Jo, S. Y. Oh and J. Park, *Biosens. Bioelectron.*, 2007, **23**, 51–59.
36. J. T. Liu, C. J. Chen, T. Ikoma, T. Yoshioka, J. S. Cross, S. Chang, J. Tsai and J. Tanaka, *Anal. Chim. Acta*, 2011, **703**, 80–86.
37. B. V. M. Silva, I. T. Cavalcanti, A. B. Mattos, P. Moura, M. D. P. T. Sotomayor and R. F. Dutra, *Biosens. Bioelectron.*, 2010, **26***,* 1062–1067.

GRAPHICAL ABSTRACT

Label-free electrochemical immunosensor based on ionic organic molecule and chitosan-stabilized gold nanoparticles for the detection of cardiac troponin T

Daniela Brondani, Jamille Valéria Piovesan, Eduard Westphal, Hugo Gallardo, Rosa Amalia Fireman Dutra, Almir Spinelli and Iolanda Cruz Vieira

A label-free electrochemical immunosensor based on an ionic organic molecule and chitosan-stabilized gold nanoparticles was developed for the detection of cardiac troponin T (cTnT).